# Highlights

Multidimensional scaling of two-mode three-way asymmetric dissimilarities: finding archetypal profiles and clustering

Aleix Alcacer, Rafael Benítez, Vicente J. Bolós, Irene Epifanio

- New multidimensional scaling of three-way proximity data
- Explicit solution, scalable, and easy interpretation
- Archetypal profiles and clustering of three-way asymmetric proximities
- For the conditional and unconditional framework

# Multidimensional scaling of two-mode three-way asymmetric dissimilarities: finding archetypal profiles and clustering

Aleix Alcacer<sup>a</sup>, Rafael Benítez<sup>b</sup>, Vicente J. Bolós<sup>b</sup>, Irene Epifanio<sup>a,\*</sup>

<sup>a</sup>Departament de Matemàtiques, Universitat Jaume I, Campus del Riu Sec, Castelló de la Plana, 12071, Spain

<sup>b</sup>Departament de Matemàtiques per a l'Economia i l'Empresa, Universitat de València, Campus de Tarongers, València, 46022, Spain

#### Abstract

Multidimensional scaling visualizes dissimilarities among objects and reduces data dimensionality. While many methods address symmetric proximity data, asymmetric and especially three-way proximity data—capturing relationships across multiple occasions—remain underexplored. Recent developments, such as the h-plot, enable the analysis of asymmetric and non-reflexive relationships by embedding dissimilarities in a Euclidean space, allowing further techniques like archetypoid analysis to identify representative extreme profiles. However, no existing methods extract archetypal profiles from threeway asymmetric proximity data. This work extends the h-plot methodology to three-way proximity data under both symmetric and asymmetric, conditional and unconditional frameworks. The proposed approach offers several advantages: intuitive interpretability through a unified Euclidean representation; an explicit, eigenvector-based analytical solution free from local minima; scale invariance under linear transformations; computational efficiency for large matrices; and a straightforward goodness-of-fit evaluation. Furthermore, it enables the identification of archetypal profiles and clustering structures for three-way asymmetric proximities. Its performance is compared with existing models for multidimensional scaling and clustering, and illustrated through a financial application. All data and code are provided to facilitate reproducibility.

<sup>\*</sup>epifanio@uji.es

#### 1. Introduction

Multidimensional scaling (MDS) comprises a series of statistical techniques used to visualize dissimilarities between a set of objects and reduce the dimensionality. Carroll and Arable (1980) proposed a taxonomy of data and defined the way and the mode. The mode indicates a set of entities, while the way represents the number of modes (with possible repetitions) that define the data array. Three-way proximity data capture relationships between pairs of entities measured across multiple occasions, such as different conditions, settings, sources, or times. They extend traditional two-way proximity data into a three-dimensional framework, where the additional dimension represents the occasion of each pairwise proximity. These data are typically organized as a series of square matrices—one per occasion—containing proximities between all object pairs, which may be symmetric or asymmetric.

A review of the literature on MDS reveals a clear imbalance: while numerous methods have been developed for symmetric proximity data, considerably less attention has been given to methods addressing asymmetric proximity data, and even less to those dealing with three-way data.

Recently, there has been a renewed interest in dimensionality reduction for asymmetric relationships, as reflected in the growing number of publications on this topic in recent years (Okada and Imaizumi, 2024; Olszewski, 2024, 2023; Di Nuzzo et al., 2025; Bove et al., 2021). A comprehensive overview of various methods for analyzing asymmetric pairwise relationships is provided by Bove and Okada (2018).

Epifanio (2013) introduced a methodology based on the h-plot, which accommodates non-metric properties such as asymmetry and lack of reflexivity (i.e., positive self-dissimilarity). The core idea is to embed the variables that define proximity to or from each object, rather than embedding the objects themselves. In the h-plot, the dissimilarity matrix is treated as a data matrix comprising two variables: the dissimilarity from element "j" to all other elements  $(d_j)$  and the dissimilarity from all other elements to "j"  $(d_j)$ . In this representation, the Euclidean distance between two variables corresponds to the sample standard deviation of their differences, where smaller values indicate higher similarity between variables. Epifanio (2014) employed that

methodology to analyze asymmetric citation relationships between a series of journals.

Projecting the data into a Euclidean space makes it possible to apply various statistical techniques, such as archetypoid analysis (ADA) (Vinué et al., 2015), as demonstrated by Vinué and Epifanio (2017). ADA is an unsupervised statistical learning method that identifies representative extreme cases, known as archetypoids, within a data set. These archetypoids are actual observations used to approximate all other data points as convex combinations of them. Because ADA relies on Euclidean distances and convex combinations, projecting the data into a Euclidean space, where these operations are meaningful, ensures the method's validity. Moreover, ADA provides a human-interpretable summary of the data, as people tend to understand and interpret extremes more intuitively.

As regards the analysis of three-way asymmetric proximity data, to the best of our knowledge, no method has been proposed yet for finding archetypal profiles in such a case.

In relation to clustering, which is another unsupervised learning methodology, although there are several methodologies for one-mode two-way asymmetric data (Olszewski, 2016), as far as we know, only three clustering methods have been proposed for the analysis of three-way asymmetric proximity data. Chaturvedi and Carroll (1994) identified two distinct yet overlapping sets of object clusters (corresponding to the rows and columns of the data matrices and shared across all occasions), which pose considerable interpretative challenges. A more parsimonious alternative is Bocci and Vicari (2024), whose model relies on two clustering structures for the objects, which are linked one-to-one and shared across all occasions. The first structure represents a standard partition of the objects, capturing the average levels of exchange, while the second represents an incomplete partition that models the imbalances by allowing certain objects to remain unassigned. Furthermore, to accommodate the heterogeneity across occasions, the magnitudes and directions of exchange between clusters are described using occasion-specific weights. A recent alternative has been proposed by Okada and Yokoyama (2025), who extended ACLUSKEW (Asymmetric Cluster analysis based on SKEW-symmetry) by Okada and Yokoyama (2015) from one-mode two-way asymmetric proximities to two-mode three-way asymmetric proximities.

Two-mode three-way data are referred to as matrix unconditional data when elements from any two different matrices can be meaningfully compared; otherwise, they are referred to as matrix conditional data. Therefore, given the absence of existing methods for finding archetypal profiles for three-way asymmetric proximity data, our research aims are as follows: First, to extend the h-plot-based methodology proposed by Epifanio (2013) to three-way proximity data, both for conditional and unconditional framework, and symmetric and asymmetric proximities; second, to use its results to obtain archetypal profiles for three-way proximity data; and third, to cluster three-way asymmetric proximities. In Sec. 2, h-plot and ADA are reviewed. Sec. 3 introduces our proposal for multidimensional scaling and finding archetypal profiles and clusters of three-way proximities. Our proposal is compared with several methodologies in Sec. 4. A real application in a financial problem is analyzed in Sec. 5. Finally, conclusions are provided in Sec. 6.

For reproducibility, codes and data are available as Supplementary Information.

# 2. Background

#### 2.1. H-plot for one-mode two-way data

H-plots were defined by Corsten and Gabriel (1976) as a method for visualizing relationships among multiple variables in a data matrix  $\mathbf{X}$ . To construct a two-dimensional h-plot, one performs an eigendecomposition of the variance–covariance matrix  $\mathbf{S}$  of  $\mathbf{X}$ . Since  $\mathbf{S}$  is positive semidefinite, all of its eigenvalues are nonnegative. Denote by  $\lambda_1$  and  $\lambda_2$  the two largest eigenvalues, and by  $\mathbf{q}_1$  and  $\mathbf{q}_2$  their corresponding unit eigenvectors. The two-dimensional h-plot is then defined as

$$\mathbf{H}_2 = \left(\sqrt{\lambda_1}, \mathbf{q}_1, \ \sqrt{\lambda_2}, \mathbf{q}_2\right).$$

The Euclidean distance between two rows,  $\mathbf{h}_i$  and  $\mathbf{h}_j$ , is approximately equal to the sample standard deviation of the difference between variables "i" and "j" (Seber, 1984). This relationship holds exactly for the full matrix  $\mathbf{H}$  defined similarly to  $\mathbf{H}_2$  but with all eigenvalues and eigenvectors. Consequently, when the two largest eigenvalues capture most of the total variance,  $\mathbf{H}_2$  provides an effective low-dimensional approximation.

Note that although eigenvectors of S are calculated, there is a clear distinction from principal component analysis (PCA). In PCA, the primary focus is on representing the n objects within the component space through the scores (the product of the data matrix and the eigenvectors). In this

space, the Euclidean distances between objects correspond exactly to their Mahalanobis distances in the original variable space.

To evaluate the adequacy of the two-dimensional h-plot, Corsten and Gabriel (1976) proposed the following goodness-of-fit measure, where values close to 1 indicate a better representation:

$$\frac{\lambda_1^2 + \lambda_2^2}{\sum_i \lambda_i^2}. (1)$$

This measure can be generalized to h-plots of any dimension and to subsets of any number of eigenvalues in a straightforward way.

Let us see how h-plot can be used for multidimensional scaling. Let  $\Delta$  be an  $n \times n$  dissimilarity matrix with elements  $\delta_{ij}$  representing the dissimilarity from object "i" to object "j". When  $\Delta$  is asymmetric, we define

$$\mathbf{D} = \left[ \boldsymbol{\Delta} | \boldsymbol{\Delta}' \right],$$

an  $n \times 2n$  matrix formed by concatenating  $\Delta$  and its transpose  $\Delta'$  columnwise, where ' denotes transposition.

When **D** is treated as a data matrix, the first n columns correspond to variables of the form  $d_{\cdot j}$ , that is, the dissimilarities from all other objects to object "j". The second block of n columns represents variables of the form  $d_{i}$ —the dissimilarities from object "j" to all other objects.

After applying h-plotting, the matrix  $\mathbf{H}_2$  contains 2n rows: the first n rows approximate the  $d_{\cdot j}$  variables, while rows n+1 through 2n approximate the  $d_{j\cdot}$  variables.

In the context of multidimensional scaling, when  $\Delta$  is symmetric h-plotting is applied to the matrix  $\Delta$ , but to  $\mathbf{D}$  if  $\Delta$  is asymmetric.

In the last case, we reverse the concatenation and partition the matrix  $\mathbf{H}_2$  into two individual blocks, each consisting of n rows, and display them. The first block corresponds with  $d_{\cdot j}$  profiles while the second block corresponds with  $d_{j\cdot}$  profiles. As regards interpretation, if two profiles,  $d_{\cdot j}$  and  $d_{\cdot i}$ , are similar, they will be positioned close to each other in the plot; the same holds analogously for the  $d_{j\cdot}$  and  $d_{i\cdot}$  profiles. Moreover, both  $d_{\cdot j}$  and  $d_{i\cdot}$  profiles are represented within a single unified space, allowing for direct comparison between them. In the symmetrical case,  $d_{\cdot j} = d_{j\cdot}$ , so we only need to represent one variable for object "j"; this is why h-plotting is applied to matrix  $\Delta$ .

In the asymmetrical case, when a  $d_{\cdot j}$  profile lies near a  $d_{j}$  profile, it indicates a high degree of similarity between the two. Consequently, the

Citing/Cited	AP	SF	SU	ТН
AP	1	10	5	10
$\operatorname{SF}$	4	2	5	10
SU	4	9	3	6
TH	10	10	7	1

Table 1: Dissimilarities between journals.

Euclidean distance between  $d_{\cdot j}$  and  $d_{j}$  profiles within this representation can be used to assess asymmetry among objects, i.e. objects whose  $d_{\cdot j}$  and  $d_{j}$  profiles are close are more symmetric, whereas greater separation reflects stronger asymmetry.

In essence, the purpose of the h-plot is not to preserve pairwise dissimilarities exactly, but rather to maintain the relationships among the dissimilarity variables, that is, the dissimilarity profiles themselves. This makes h-plotting particularly useful for analyzing non-metric dissimilarities, where an exact Euclidean representation is not feasible due to the inherently non-Euclidean nature of the proximities.

If our goal is cluster or pattern detection, expanding or contracting the configuration may be more informative (Seber, 1984). Therefore, we can replace the actual dissimilarity values with their corresponding ranks instead (Borg and Groenen, 2005; Okada and Imaizumi, 2024). Similarly, other transformations—such as raising the dissimilarities to a power—can also be applied (Podani and Miklós, 2002).

#### 2.1.1. Toy example

For illustrative purposes, we consider the dissimilarities between four journals: an applied statistics one (AP), a journal of a specific statistical field (SF), a journal about statistical surveys (SU), and a theoretical statistical journal (TH), shown in Table 1. This dissimilarity matrix is asymmetric and nonreflexive, since it is based on the number of citations between journals. Note that a small dissimilarity between journals i and j ( $d_{ij}$ ) indicates that journal i cites journal j extensively. Cross-journal citations exhibit clear asymmetry: journal i may not cite journal j to the same extent that j cites i. The triangle inequality may also fail, and self-citation indicates non-reflexivity.

Fig. 1 displayed the h-plot projection of Table 1. The goodness of fit for the first dimension is 80.17%, while it is 99.85% for the two dimensions.

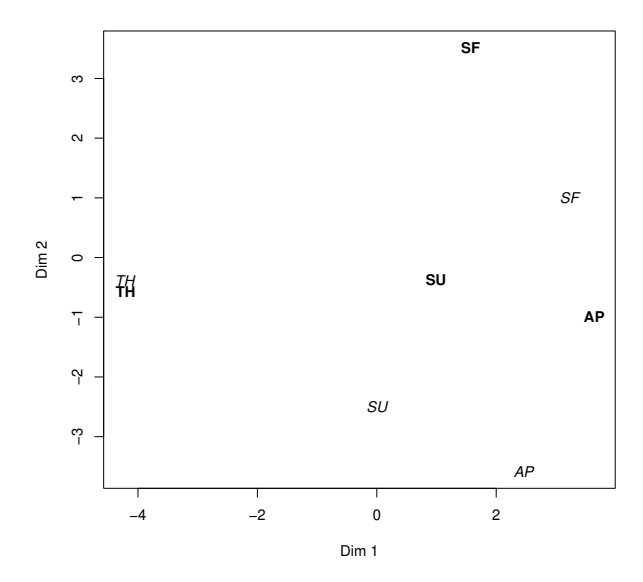


Figure 1: H-plot projection of one-mode two-way journal citation data. Bold font represents the dissimilarity variables of cited  $(d_{ij})$ , while italic font denotes citing  $(d_{ji})$ .

The more applied journals are situated on the right part of the plot, while the theoretical journal is on the left-hand side. To assess the asymmetry for each journal, we compute the Euclidean distance between the h-plot representation of each journal as citing and cited. The most symmetrical journal (the journals that cite are similar to the journals that cited it) is TH, the theoretical journal; while the most asymmetrical journal is SF, whose cites come from different journals than those that the SF journal cites.

Although the most citing and cited journal for SF is SF (the dissimilarity is 2), the nearest profile of SF citing profile is the cited AP profile, i.e., the journals that SF cites are more similar to the journals that cite AP. This is because the h-plot does not aim to reproduce pairwise dissimilarities directly, but rather to represent each object's relationships with all others.

#### 2.1.2. Advantages of h-plots

H-plots offer several notable benefits:

1. Intuitive interpretability: Profiles are directly comparable since all profiles are displayed within a single, unified Euclidean representation.

- 2. Explicit solution: They provide a direct analytical solution based on eigenvectors, avoiding the problem of local minima that often arises in iterative optimization methods. Furthermore, the resulting configuration remains consistent even when the roles of objects and individuals are interchanged.
- 3. Scale invariance: h-plots are invariant under linear transformations of the dissimilarity scale, meaning that changes in scale do not affect the overall visual configuration (Epifanio, 2013).
- 4. Computational efficiency: They are computationally efficient and capable of handling very large matrices, making them a scalable approach (Schwarz and Karlsson, 2019).
- 5. Simple goodness-of-fit evaluation: The quality of the representation can be easily quantified using the clear goodness-of-fit measure given by (1).
- 6. Robustness: When outliers are present, robust variants of h-plots can be computed, as proposed by Daigle and Rivest (1992).

# 2.2. Partitioning around medoids (PAM)

The k-medoids algorithm identifies k representative observations within each cluster, referred to as medoids (Kaufman and Rousseeuw, 1990), from the data set such that the total within-cluster dissimilarity is minimized, i.e., medoids correspond to actual data points from the original data set. It is defined for symmetrical dissimilarity matrices.

For a given k, k-medoids searches k observations of the data,  $i_1^*$ , ...,  $i_k^*$  such that

$$\{i_1^*, \dots, i_k^*\} = \underset{\mathbf{Y}, \mathbf{i_1}, \dots, \mathbf{i_k}}{\arg\min} \sum_{i \in \mathbf{Y}} \inf_{1 \le j \le k} \delta_{ii_j}, \tag{2}$$

where **Y** ranges on subsets of observations indexed from 1 to n. It can be computed with the function pam from the R (R Development Core Team, 2025) package cluster (Maechler et al., 2025). This function also returns the silhouette information. The number of clusters for which the silhouette coefficient is maximum can be considered as the best choice of k (Kaufman and Rousseeuw, 1990). If the average silhouette width exceeds 0.7, the clustering is regarded as strong; values near 0.5 indicate a reasonable solution, while those near 0.25 are generally viewed as weak.

# 2.3. Archetypoid Analysis

ADA is founded on the premise that data can be expressed as convex combinations of a small set of archetypal patterns drawn directly from the data set itself (see Alcácer et al. (2025) for a comprehensive overview). In statistics, archetypal profiles carry the same intuitive meaning as in everyday language, i.e., they represent extreme or pure types. Archetypal patterns are more readily interpretable than central or average points, as people tend to understand data more intuitively through contrasting or opposing examples (Thurau et al., 2012).

Let 
$$\mathbf{X} = \begin{pmatrix} \mathbf{x}_1 \\ \vdots \\ \mathbf{x}_n \end{pmatrix}$$
 denote an  $n \times m$  data matrix containing  $n$  observations

and m variables. In ADA, three matrices are introduced to approximate the underlying data structure through mixtures (i.e. convex linear combinations) of representative observations:

- 1. Archetypoids: The k archetypoids, denoted by  $\mathbf{z}_j$ , form the rows of a  $k \times m$  matrix  $\mathbf{Z}$ . Each  $\mathbf{z}_j$ , for  $j = 1, \ldots, k$ , corresponds to one specific case from the original data matrix  $\mathbf{X}$ .
- 2. Mixture coefficients: The  $n \times k$  matrix  $\boldsymbol{\alpha} = (\alpha_{ij})$  contains the coefficients used to approximate each observation  $\mathbf{x}_i$  as a mixture of the archetypoids:

$$\mathbf{x}_i \approx \hat{\mathbf{x}}_i = \sum_{j=1}^k \alpha_{ij} \mathbf{z}_j, \tag{3}$$

where  $\alpha_{ij} \geq 0$  and  $\sum_{j=1}^{k} \alpha_{ij} = 1$  for  $i = 1, \dots, n$ .

3. Selection matrix: The  $k \times n$  matrix  $\boldsymbol{\beta} = (\beta_{jl})$  is composed of binary coefficients that identify which observations are chosen as archetypoids. Each archetypoid  $\mathbf{z}_j$  is defined as

$$\mathbf{z}_j = \sum_{l=1}^n \beta_{jl} \mathbf{x}_l,\tag{4}$$

where  $\beta_{jl} \in \{0,1\}$  and  $\sum_{l=1}^{n} \beta_{jl} = 1$  for  $j = 1, \dots, k$ , so it is guaranteed that each archetypoid corresponds to an actual case in **X**.

From (3) and (4), the Residual Sum of Squares (RSS) is given by

$$RSS = \sum_{i=1}^{n} (\mathbf{x}_i - \hat{\mathbf{x}}_i)^2 = \sum_{i=1}^{n} \left( \mathbf{x}_i - \sum_{j=1}^{k} \alpha_{ij} \sum_{l=1}^{n} \beta_{jl} \mathbf{x}_l \right)^2.$$
 (5)

The goal is to solve the following mixed-integer optimization problem, taking into account expression (5):

$$\min_{\boldsymbol{\alpha},\boldsymbol{\beta}} RSS(\boldsymbol{\alpha},\boldsymbol{\beta}) \tag{6}$$
s.t. 
$$\sum_{j=1}^{k} \alpha_{ij} = 1, \qquad i = 1, \dots, n, \quad \text{Convexity}$$

$$\sum_{l=1}^{n} \beta_{jl} = 1, \qquad j = 1, \dots, k, \quad \text{Binary assignment}$$

$$\alpha_{ij} \geq 0, \, \beta_{jl} \in \{0, 1\}.$$

Program (6) is solved using the two-phase algorithm introduced by Vinué et al. (2015). In the first phase, known as BUILD, an initial solution is generated by selecting a preliminary set of candidate archetypoids. The second phase, termed SWAP, iteratively refines this set by exchanging selected archetypoids with unselected observations whenever such replacements lead to a reduction in the RSS. Our analysis employs the R implementation developed by Epifanio et al. (2018).

To decide the proper number of archetypoids, we adopt the elbow criterion, as used in prior studies such as Cutler and Breiman (1994); Eugster and Leisch (2009); Vinué et al. (2015). This method entails plotting the RSS against the number of archetypoids and identifying the point where the rate of decrease in RSS markedly diminishes, commonly referred to as the "elbow".

#### 2.4. H-plot + ADA for one-mode two-way data

For symmetrical relationships, ADA can be applied to the h-plot projections, since they are in an Euclidean space. As archetypoids are sample points, the representative points are univocally identified. The ADA method has been successfully combined with h-plot projection in several previous studies. For instance, Epifanio et al. (2023) applied it to the analysis of foot shapes, while Alcácer et al. (2021) used it in a shoe size recommendation system, and Epifanio et al. (2020) employed it across various data sets containing

missing data. Additionally, Vinué et al. (2015) applied the methodology to non-metric but symmetric dissimilarities derived from 3D binary images of the trunks of Spanish women for apparel design. In the same work, Vinué et al. (2015) conducted a simulation study using non-metric yet symmetric dissimilarities to evaluate which MDS technique most effectively recovered archetypoids after projection. The h-plot method was compared with six other MDS techniques—Classical (Metric) MDS, Kruskal's Non-metric MDS, Sammon's Nonlinear Mapping, Isomap (Tenenbaum et al., 2000), Locally Linear Embedding (Roweis and Saul, 2000), and Diffusion Map (Nadler et al., 2006)—and demonstrated superior performance in recovering the original archetypoids.

In the case of asymmetric relationships, Vinué and Epifanio (2017) proposed the application of ADA to two-dimensional h-plot projections as well. It is important to note that each object j has two associated profiles: one corresponding to  $d_j$  and another approximating  $d_j$ . Both profiles are represented within the same configuration by the two-dimensional vectors  $\mathbf{h}_j$  and  $\mathbf{h}_{j+n}$ , for  $j=1,\ldots,n$ . Consequently, ADA is applied to an  $n\times 4$  matrix  $\mathbf{X}$ , constructed by combining the representations from both blocks of h-plot profiles. Specifically, the j-th row of  $\mathbf{X}$  consists of the concatenated vectors  $\mathbf{h}_j$  and  $\mathbf{h}_{j+n}$ .

#### 3. Methodology

Assume that  $\Delta_l$  (l = 1, ..., L) denotes a square dissimilarity matrix, where each element  $\delta_{ijl}$  corresponds to the pairwise dissimilarity from object i to object j (i, j = 1, ..., n) observed at occasion or condition l. If  $\delta_{ijl} = \delta_{jil}$ , the dissimilarity matrix is said to be symmetric; otherwise, it is considered asymmetric.

#### 3.1. Multidimensional scaling for unconditional two-mode three-way data

In this section, we consider unconditional matrices, where the entries are directly comparable across the entire set of matrices.

For the symmetric case, we define

$$\mathbf{D} = \left[ \mathbf{\Delta}_1 | ... | \mathbf{\Delta}_L \right],$$

as an  $n \times Ln$  matrix formed by concatenating  $\Delta_l$  matrices column-wise.

Then, **D** is h-plotted in two dimensions, obtaining thus the matrix  $\mathbf{H}_2$  with Ln rows and two columns. Next, we divide  $\mathbf{H}_2$  into L blocks of n rows

	(	Occas	sion	1	Occasion 2				
		В							
A	50	25	50	25	50	50	19	23	
В	50	0	50	25	18	25	10	10	
$\mathbf{C}$	20	20	50	10	50	50	0	20	
D	20	25 0 20 10	20	0	27	22	5	0	

Table 2: Artificial three-way proximity data.

and rearrange them into a matrix  $\mathbf{Y}$  consisting of n rows and 2L columns, i.e., L matrices of size  $n \times 2$  stacked columnwise. Each of the L blocks is visualized in a two-dimensional plot, with distinct colors indicating the different conditions.

For the asymmetric case, we define

$$\mathbf{D} = \left[ \mathbf{\Delta}_1 \, | \, \mathbf{\Delta}_1' \, | \, \dots \, | \, \mathbf{\Delta}_L \, | \, \mathbf{\Delta}_L' \right],$$

as an  $n \times 2Ln$  matrix formed by concatenating the matrices  $\Delta_l$  and their transposes  $\Delta'_l$  column-wise.

Then, **D** is h-plotted in two dimensions, obtaining the matrix  $\mathbf{H}_2$  with 2Ln rows and two columns. We reverse the concatenation and partition the matrix  $\mathbf{H}_2$  into individual blocks, each consisting of n rows. Each of the 2L blocks is visualized in a two-dimensional plot, with L distinct colors indicating the different conditions, and with two different font styles: bold and italic for  $d_{\cdot jl}$  and  $d_{j\cdot l}$  profiles, respectively. This new matrix, denoted as  $\mathbf{Y}$ , consists of n rows and 4L columns.

#### 3.1.1. Illustrative example

Let us consider in Table 2 a three-way array representing pairwise exchanges of messages among n=4 people in L=2 occasions. Note that proximities are asymmetric, and the reflexive property is not fulfilled. Similarities are converted into dissimilarities by subtracting 50, i.e., the maximum value in the matrices. Considering that entries are comparable in both occasions,  $\mathbf{D}$  is arranged as a  $4\times 16$  matrix in Table 3. Fig. 2 displayed the h-plot projection.

On the one hand, dimension 1 is related to interactions with individuals B and C. The further to the right, the less interaction with B and the more with C; while the further to the left, the more interaction with B and the less with C. On the other hand, dimension 2 measures interactions with A:

	I	Recei	ved 1	1	;	Send	ing 1		I	Recei	ved :	2		Send	ing 2	2
	A	В	С	D	Α	В	С	D	A	В	С	D	A	В	С	D
A	0	25	0	25	0	0	30	30	0	0	31	27	0	32	0	23
В	0	50	0	25	25	50	30	40	32	25	40	40	0	25	0	28
С	30	30	0	40	0	0	0	30	0	0	50	30	31	40	50	45
D	30	40	30	50	25	25	40	50	23	28	45	50	27	40	30	50

Table 3: Matrix **D** for the unconditional two-mode three-way artificial example. "Received" means  $d_{\cdot j}$  profiles, while "Sending" denotes  $d_{j}$ . profiles, and numbers indicate the occasions 1 and 2.

the more interactions, the lower the position, and the fewer interactions, the higher the position.

The most similar profiles, those that are nearest in h-plot configuration, are received by D in occasion 2 and sent by D in occasion 1.

As regards asymmetry, the most symmetric profile is D in occasion 1, while the most asymmetrical is A in occasion 2, i.e., the received and sending profiles for D in occasion 1 are the most similar, but they are the least similar for A in occasion 2.

#### 3.2. Multidimensional scaling for conditional two-mode three-way data

In this section, we consider conditional matrices, where entries are comparable within each specific condition or occasion (e.g., within a single participant's ratings), but not across different conditions or occasions. As the conditions are not comparable, they cannot be considered as different dissimilarity variables as in Sect. 3.1 and conditions will not be displayed separately. Conditions will be treated as distinct observations of the dissimilarity variables. Since the covariances between the dissimilarity variables are computed to construct the h-plot, the comparisons in the same row are valid.

For the symmetric case, we define

$$\mathbf{D} = egin{bmatrix} oldsymbol{\Delta}_1 \ ... \ oldsymbol{\Delta}_L \end{bmatrix}$$

as an  $Ln \times n$  matrix formed by concatenating  $\Delta_l$  matrices row-wise.

Then, **D** is h-plotted in two dimensions, obtaining the matrix  $\mathbf{H}_2$  with n rows and two columns. This h-plot projection, denoted by  $\mathbf{Y}$ , consists of n rows and 2 columns.

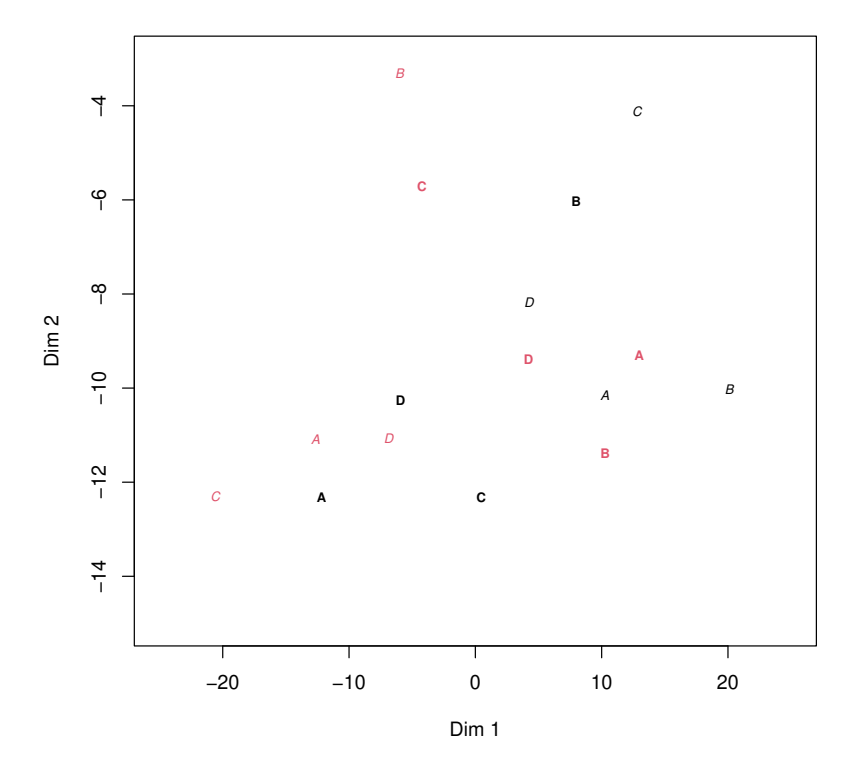


Figure 2: H-plot projection of unconditional two-mode three-way artificial example. The first condition is represented in black, and the second in red. See the text for the meaning of the bold and italic fonts.

For the asymmetric case, we define

$$\mathbf{D} = egin{bmatrix} oldsymbol{\Delta}_1 & oldsymbol{\Delta}_1' \ ... \ oldsymbol{\Delta}_L & oldsymbol{\Delta}_L' \end{bmatrix}$$

as an  $Ln \times 2n$  matrix formed by concatenating the matrices  $\Delta_l$  and their transposes  $\Delta'_l$  row-wise.

Then, **D** is h-plotted in two dimensions, obtaining the matrix  $\mathbf{H}_2$  with 2n rows and two columns. We reverse the concatenation and partition the matrix  $\mathbf{H}_2$  into two individual blocks, each consisting of n rows. Each of the two blocks is visualized in a two-dimensional plot, with two different font

	Received				Sending			
Occasion 1	A	В	С	D	A	В	С	D
A	0	25	0	25	0	0	30	30
В	0	50	0	25	25	50	30	40
С	30	30	0	40	0	0	0	30
D	30	40	30	50	25	25	40	50
Occasion 2	A	В	С	D	A	В	С	D
A	0	0	31	27	0	32	0	23
В	32	25	40	40	0	25	0	28
$^{\mathrm{C}}$	0	0	50	30	31	40	50	45
D	23	28	45	50	27	40	30	50

Table 4: Matrix **D** for the conditional two-mode three-way artificial example.

styles: bold and italic for  $d_{\cdot j}$  and  $d_{j}$  profiles, respectively. This new matrix, denoted as  $\mathbf{Y}$ , consists of n rows and 4 columns.

#### 3.2.1. Illustrative example

Data in Table 2 is considered. Again, similarities are converted into dissimilarities by subtracting 50 to all entries in the matrix. Now, we consider that the entries in both occasions are not comparable, therefore  $\mathbf{D}$  is arranged as an  $8 \times 8$  matrix as shown in Table 4. Its h-plot is displayed in Fig. 3.

The first dimension is related to interactions with individual C. The further to the right, the less interaction with C in occasion 1 and the more with C in occasion 2; while the further to the left, the more interaction with C in occasion 1 and the less in occasion 2. On the other hand, dimension 2 measures interactions with A and B: the fewer interactions in occasion 1 and the more interactions in occasion 2, the higher the position, and conversely, the more interactions with A and B in occasion 1 and the fewer in occasion 2, the lower the position.

The most similar profiles, those that are nearest in h-plot configuration, are sent by A and sent by C.

Regarding asymmetry, the most symmetric profile is D, while the most asymmetrical is C. Specifically, the received and sending profiles for D are the most similar, whereas they are the least similar for C.

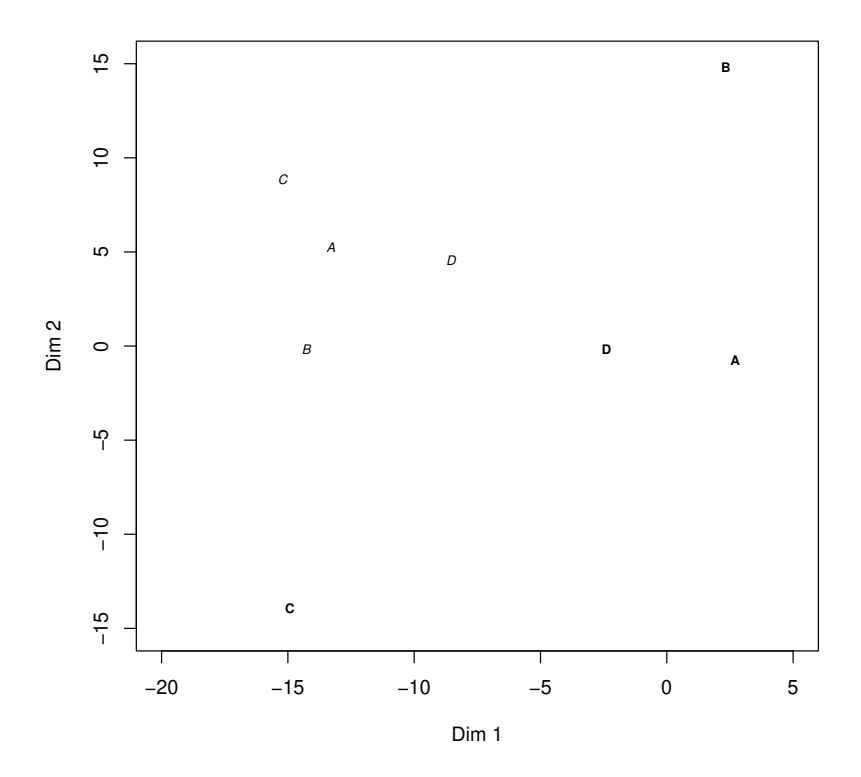


Figure 3: H-plot projection of conditional two-mode three-way artificial example. See the text for the meaning of the bold and italic fonts.

#### 3.3. Archetypal profiles for two-mode three-way data

In an analogous way to that in Sect. 2.4, ADA is applied to the matrix **Y**, which is different for unconditional and conditional two-mode three-way data. As Euclidean space is considered in h-plotting projection, ADA can be computed validly.

# 3.4. Clustering for two-mode three-way data

Similarly, as explained in Sect. 3.3, we can applied a clustering method to matrix  $\mathbf{Y}$ . We consider PAM for obtaining medoids, which are representative points, like the alter ego of archetypoids for clustering.

#### 4. Comparison with other methodologies

In this section, the proposed methodologies are compared with several existing alternative approaches using three different problems analyzed previously in the literature.

#### 4.1. Illustrative example

Data in Table 2 is analyzed by two-mode three-way radius-distance model developed by Okada and Imaizumi (1997), which is matrix conditional. Fig. 4 shows the results. The common object configuration shown in this figure reveals similar symmetric relationships among the objects. Radii reveal asymmetry. The most asymmetric person is C, which coincides with the h-plot results shown in Figure 3, but not with the most symmetrical case, as here the radius of B is zero. Note that, unlike in the radius-distance model, with the h-plot, we have access to the information about sent and received profiles.

#### 4.2. Asian Nation Data

The following example was thoroughly analyzed by Okada and Imaizumi (2024). The data set comprises two  $10 \times 10$  asymmetric similarity matrices (i.e.,  $10 \times 10 \times 2$  two-mode, three-way similarity data) representing relationships among 10 Asian countries. In each matrix, the element at position (j, i) of the l-th matrix denotes the mean rating—provided by respondents in nation j—of the influence exerted by nation i on nation j during year l. A larger value in the (j, i) cell indicates that respondents in nation j perceived the influence of nation i on their own nation more positively or favorably in that year. Okada and Imaizumi (2024) analyzed this data set using the two-mode three-way radius-distance model developed by Okada and Imaizumi (1997), which is matrix conditional, and INDSCAL (Carroll and Chang, 1970), which assumes symmetry and therefore cannot model asymmetric relationships.

Fig. 5 shows the results with the radius-distance model. Korea has the smallest radius, equal to zero, indicating that respondents in Korea consistently evaluate the influence of other nations on Korea as more negative or less favorable than Korea's influence on them. In contrast, the Philippines has the largest radius, suggesting that respondents there tend to rate the influence of other nations on the Philippines as more positive or favorable

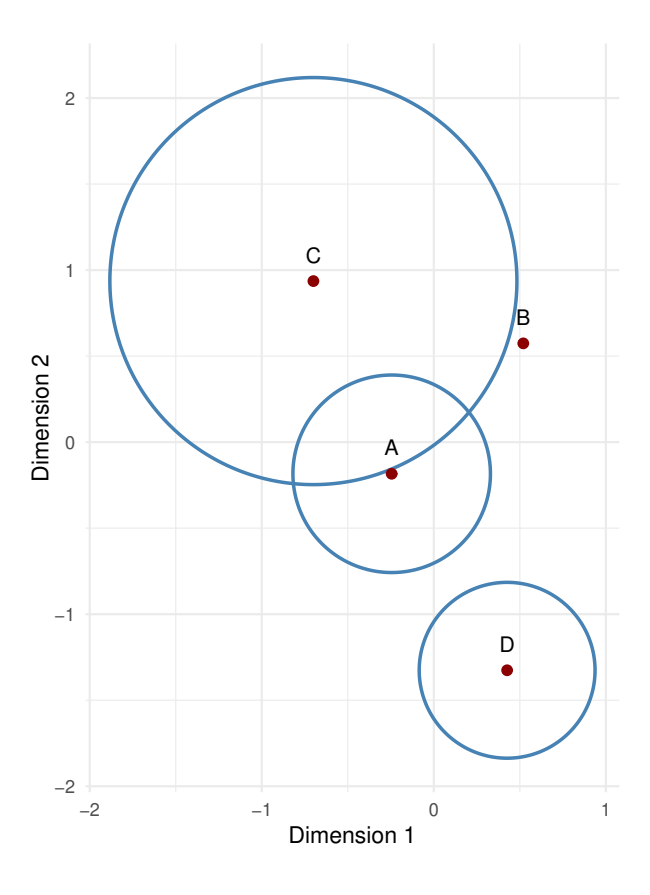


Figure 4: Two-dimensional common object configuration of illustrative example in Sec. 3.2.1 by radius-distance model.

than the reverse. The correlation coefficients of GDP and each dimension and radius are -0.5, -0.61, and -0.34, respectively.

Although our model can work with conditional and unconditional matrices, we will show only the h-plot projection for the conditional case, in order to make a fair comparison with the results produced by the radius-distance model. Fig. 6 shows the h-plot for this data set. The goodness of fit for two dimensions is 78%, while the first dimension explains 61%. The correlation between GDP and the first h-plot dimension is 0.64 for the influencing profiles, and 0.58 for the influenced ones. The most symmetric country is Korea, while the most asymmetric are Malaysia and the Philippines (both tied). The most similar profiles are the influencing from Malaysia, Singapore, and Thailand.

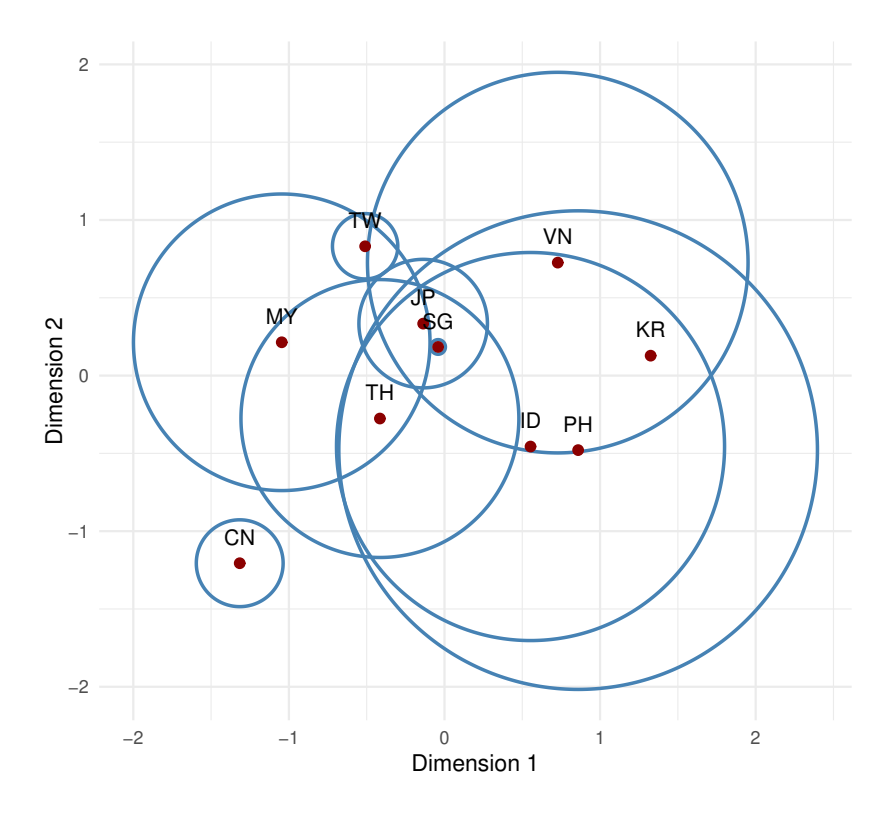


Figure 5: Two-dimensional common object configuration of nation data set by radius-distance model.

Results that emerge from Figs. 5 and 6 have coincidences, although there are also some differences worth mentioning. For example, Japan profiles are somewhat separated from the rest of the countries in the h-plot, something that does not happen with the radius-distance model.

#### 4.3. Student Mobility Data

This data set was subjected to detailed analysis by Bocci and Vicari (2024). The data used in this study come from the OECD Education Statistics Database, which provides annual information on international student exchanges in tertiary education. The data set comprises five asymmetric matrices representing student mobility among 20 OECD founding countries from 2016 to 2020. Each matrix records the number of students moving from an origin country to a host country for tertiary studies. For each year,

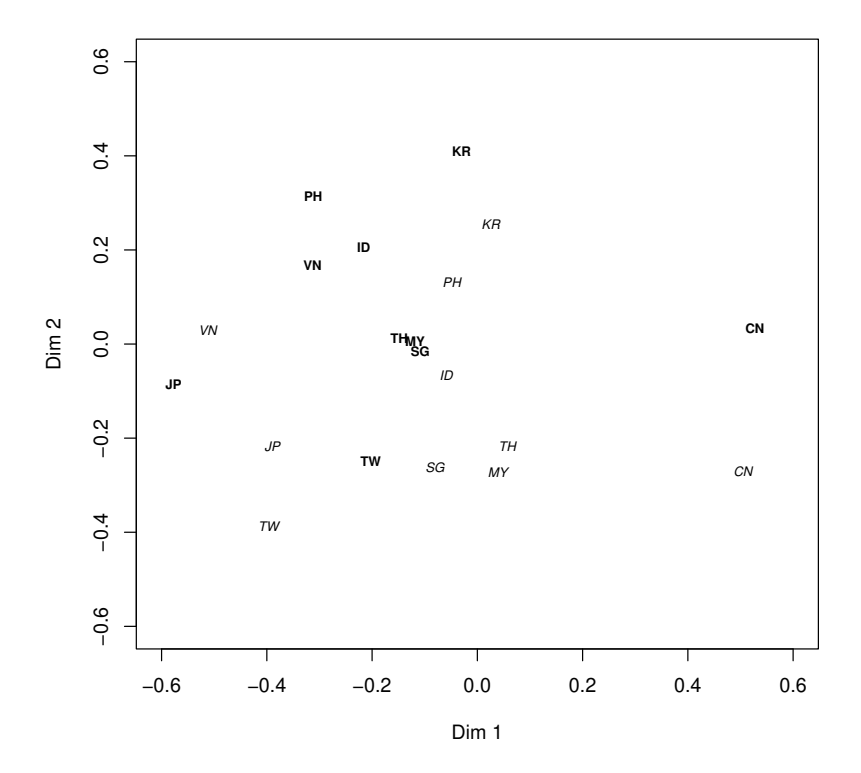


Figure 6: H-plot projection of nation data set. Bold font represents influencing  $(d_{i\cdot})$  profiles, while italic font denotes influenced  $(d_{\cdot i})$  profiles.

the proportions of outgoing students were converted into pairwise dissimilarities by calculating 100 minus each proportion. The countries are the twenty founding members of the OECD: Austria (AT), Belgium (BE), Canada (CA), Denmark (DK), France (FR), Germany (DE), Greece (EL), Iceland (IS), Ireland (IE), Italy (IT), Luxembourg (LU), Netherlands (NL), Norway (NO), Portugal (PT), Spain (ES), Sweden (SE), Switzerland (CH), Turkey (TR), United Kingdom (UK), and United States of America (US).

Bocci and Vicari (2024) computed 6 clusters, composed by: 1) DE, US; 2) EL, IE, TR; 3) DK, IS, NO, SE; 4) BE, FR, LU, NL, PT, ES; 5) AT, CA, IT, CH; and 6) UK.

We have calculated the clustering of the unconditional two-mode threeway data following the procedure described in to Sect. 3.4. According to the

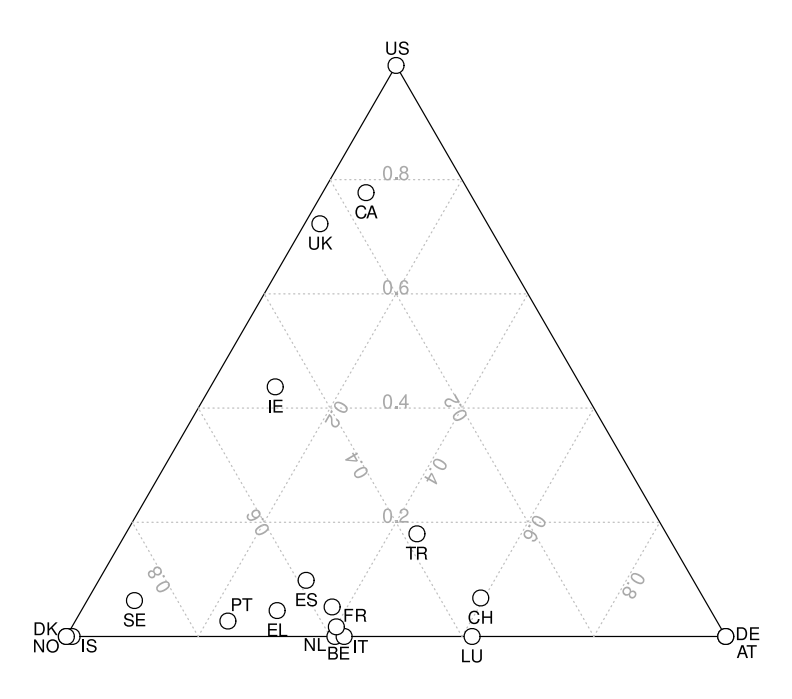


Figure 7: Ternary plot of alpha values of ADA for student mobility data.

silhouette information, the best k is 4, with 0.53 of silhouette coefficient. For comparison purposes with Bocci and Vicari (2024)'s results, we provide the results for k=4 and 6. Medoids of each group appear first. For k=4, the clusters obtained are: 1) DE, AT; 2) FR, BE, EL, IT, LU, NL, PT, ES, CH, TR; 3) UK, CA, IE, US; 4) NO, DK, IS, SE. For k=6, the clusters obtained are: 1) DE, AT; 2) IT, BE, LU, NL, CH; 3) UK, CA, US; 4) NO, DK, IS, SE; 5) ES, PO, TR; 6) IE.

Results returned by our proposal seem more geographically coherent than those returned by Bocci and Vicari (2024)'s methodology, since a cluster composed of DE and US, or being CA together with IT or CH, or IE with EL and TR are unexpected results.

We have also estimated the archetypoids following the procedure proposed in Sect. 3.3. According with the screeplot, the best k is 3. Alpha values are displayed in a ternary plot in Fig. 7. The archetypoids are: NO (and DK); AT (and DE), and US. The rest of the countries are approximated by mixtures of these archetypoids. For example, BE is a mixture of 59% NO and 41% AT; UK is a mixture of 25% NO, 2% AT, and 72% US.

#### 4.4. Cultural Participation Data

This data set was analyzed in detail by Okada and Yokoyama (2025). The data set consists of  $9 \times 9 \times 7$  two-mode, three-way asymmetric similarity matrices that describe cultural participation relationships. Each matrix represents how participation in one cultural activity relates to another across seven social groups. The nine cultural activities included are (we denote the labels for each activity in parentheses): (a) Classical music performances and concerts (Classic), (b) Museum and art exhibitions (Museum), (c) Hobby and cultural lessons (Lesson), (d) Travel abroad (Abroad), (e) Volunteer activities (Volunteer), (f) Public library use (Library), (g) Reading novels or history books (Novels), (h) Karaoke (Karaoke), (i) Reading tabloid papers and celebrity magazines (Tabloid).

The two-mode three-way ACLUSKEW developed by Okada and Yokoyama (2025) is matrix unconditional. They considered two clusters, whose dominant objects are Tabloid and Novels, which are shared across all social groups. The former represents lowbrow culture, while the latter reflects a middlebrow orientation.

We have calculated the clustering of the unconditional two-mode three-way data following the procedure described in to Sect. 3.4. We consider two groups for each social group for comparison purposes. Table 5 displays ACLUSKEW's results, the dominance objects for ACLUSKEW, and the medoids for PAM are indicated in bold.

The ACLUSKEW results show single-member clusters for four social groups. By contrast, our proposal produces more balanced results in terms of the number of elements. Furthermore, our clusters are more consistent between groups.

We have also estimated the clusters for k=2 without differencing between groups. In this case, members of each group are (medoids are in bold font): 1) **Abroad**, Lessons, Volunteer; and 2) **Novels**, Classic, Museum, Library, Karaoke, Tabloid. Nevertheless, according to the silhouette information, the best k is 3 with a silhouette coefficient of 0.49. The members of each group are: 1) **Abroad**, Lessons, Volunteer; and 2) **Novels**, Museum, Library, Karaoke, Tabloid; 3) **Classic**.

We have also estimated the archetypoids following the procedure proposed in Sect. 3.3. According to the screeplot, the best k is 3. The archetypoids are: Volunteer, Tabloid, and Classic. If we assign each activity to the archetypoid with the highest  $\alpha$  value, the groups obtained coincide with those provided by PAM.

#### 5. Application to financial products

The data set for this application corresponds to that used in Ferrer et al. (2021), consisting of daily closing prices of green bonds and equities, as well as some conventional asset classes that represent investment alternatives. Specifically, we consider the following equity indices from the NAS-DAQ OMX Green Economy family: Solar Energy (GRNSOLAR), Wind Energy (GRNWIND), Fuel Cell (GRNFUEL), Energy Efficiency (GRNENEF), Clean Transportation (GRNTRN), Green Buildings (GRNGB) and Pollution Prevention (GRNPOL). Moreover, we also consider the S&P Green Bond Index (SPGBI) and some conventional asset classes: S&P GSCI Gold (GOLD), Brent oil price (OIL) and MSCI World Index (MSCI). Finally, the global Treasury, investment-grade, and high-yield corporate bond markets are proxied by the Bloomberg Barclays Global Treasury Total Return Index (TREAS), the Bloomberg Barclays Aggregate Corporate Bond Index (IG-BOND), and the Bloomberg Barclays Global High Yield Corporate Total Return Index (HYBOND). See Ferrer et al. (2021) for a full description of these financial products.

Asymmetric dissimilarities ranging from 0 to 1 are computed using the oriented squared wavelet coherence introduced by Ferrer et al. (2021), which is based on the squared wavelet coherence and the wavelet phase-difference (Torrence and Webster, 1999). These dissimilarities are defined in terms of causality, such that if "i" influences "j", then the dissimilarity from "i" to "j" is smaller than the dissimilarity from "j" to "i". Three sub-periods associated with some major financial, economic, and even health-related events are examined: the European sovereign debt crisis (13 October 2010 to 31 July 2012), the oil price collapse (20 June 2014 to 28 February 2016), and the 2020 COVID-19 pandemic (1 January to 13 November 2020). We have considered a scale interval of more than 22 days, which captures long-term interactions. The reason is that relationships between asset markets over longer time periods are less affected by short-lived phenomena, such as shifts in investor sentiment or psychological factors, than relationships over shorter time periods.

Therefore, our data are composed of a three-way data array consisting of three asymmetric dissimilarity matrices (each of which considers a different sub-period) of 14 observations.

#### 5.1. Results

We have computed the h-plot (see Fig. 8) for the unconditional two-mode three-way data. The goodness of fit is 94%. The green stocks are clustered on the right part of the plot, together with OIL and HYBOND, in accordance with the clusters obtained by Ferrer et al. (2021) for the long term. Furthermore, we can observe that these products are a bit shifted between each sub-period. On the one hand, the most asymmetrical profiles are OIL and HYBOND. Since, in most cases, the dissimilarities from OIL to the other assets are greater than the dissimilarities from the other assets to OIL (mainly in the second and third sub-periods), we can conclude that OIL influences others (particularly green stocks) more than it is influenced by them. In contrast, the dissimilarities from HYBOND to the other assets are less than the dissimilarities from the other assets to HYBOND, concluding that HYBOND is influenced more than it influences. On the other hand, the less asymmetrical profiles are TREAS and GRNFUEL. This suggests that these assets are not closely linked to the others in terms of cause and effect.

Archetypoids are calculated following the procedure proposed in Sect. 3.3. According to the screeplot, the best k is 4, being the archetypoids: TREAS, IGBOND, MSCI, and GRNFUEL. The remaining assets are estimated to be a mixture of these archetypoids. For example, GOLD is expressed as 70% TREAS and 30% GRNFUEL. Furthermore, the green stocks are mainly a mixture of GRNFUEL and MSCI, with GRNFUEL having a greater weighting. This mixture is not surprising, given that green equities represent a significant proportion of the overall equity market as measured by the MSCI index.

#### 6. Conclusions

We have extended the h-plot methodology for multidimensional scaling to the analysis of three-way proximity data, encompassing both symmetric and asymmetric as well as conditional and unconditional frameworks. While traditional MDS methods focus primarily on symmetric data, the proposed approach effectively addresses the challenges posed by asymmetric and threeway proximities, which have remained largely unexplored.

The extended h-plot framework offers several notable advantages: intuitive interpretability within a unified Euclidean representation; an explicit, eigenvector-based analytical solution that avoids local minima; scale invari-

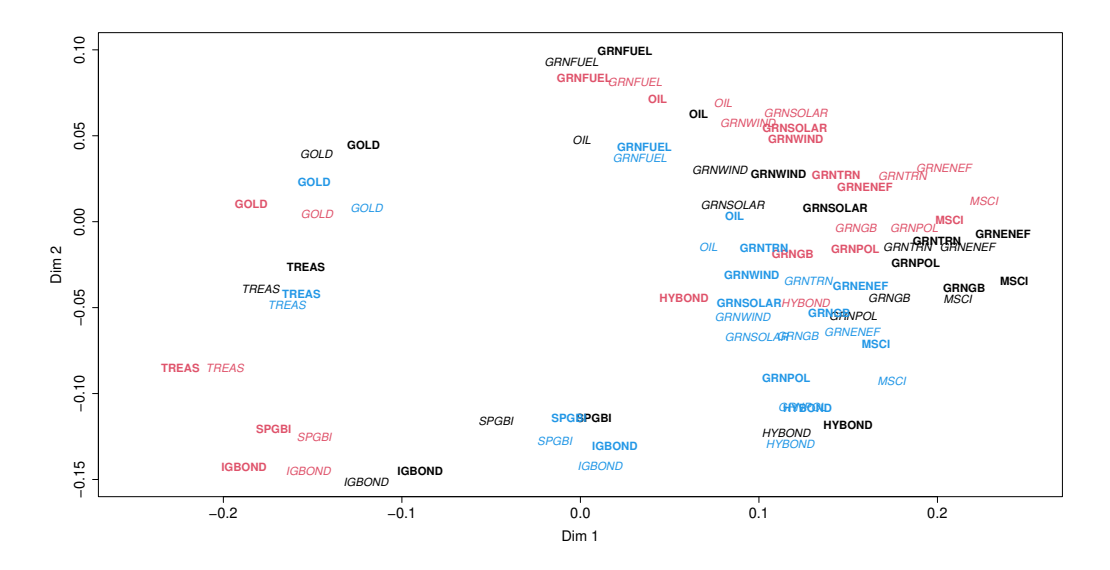


Figure 8: H-plot projection of financial products data set. Bold font represents influencing  $(d_{i\cdot})$  profiles, while italic font denotes influenced  $(d_{\cdot i})$  profiles. The first sub-period is represented in black, the second in red, and the third in blue.

ance under linear transformations; high computational efficiency for large data sets; and a simple, quantitative goodness-of-fit assessment.

Moreover, the proposed methodology facilitates the identification of archety-pal profiles and clustering structures for three-way asymmetric proximities, enhancing interpretability and analytical flexibility. Comparative analyses with existing MDS and clustering approaches, supported by a financial application, demonstrate its effectiveness. All data and code are made publicly available to ensure full reproducibility and transparency.

Several avenues for future research emerge from this work. On the one hand, some extensions to the methodology to other kinds of data. One promising direction involves representing symbolic dissimilarities using h-plots. In many applications, exact dissimilarities may be unavailable, while partial information—such as their range (Groenen et al., 2006) or distribution in the form of histograms (Groenen and Winsberg, 2006)—is accessible. For instance, interval dissimilarities could be visualized through h-plots by adapting the principles proposed by D'Enza et al. (2021). As regards missing values in the proximity matrices, several alternatives could be explored, as this problem has been considered in PCA (Gómez-Sánchez et al., 2024). On

the other hand, a promising line of future research lies in the application of the proposed methodology to practical problems across various fields, such as economics and finance or psychology. Finally, a modification of biarchety-pal analysis (Alcácer et al., 2024) could be developed to identify archetypal profiles within proximity data.

# Acknowledgments

A. Alcácer, V. J. Bolós, and I. Epifanio acknowledge financial support from the Conselleria d'Educació, Cultura, Universitats i Ocupació of the Generalitat Valenciana through Project CIPROM/2023/066. R. Benítez and V. J. Bolós acknowledge financial support from the Spanish Ministry of Science, Innovation and Universities through Project PID2023-153128NB-I00. A. Alcácer and I. Epifanio acknowledge financial support from from the Spanish Ministry of Science, Innovation and Universities through Projects PID2020-118763GA-I00 and PID2022-141699NB-I00.

#### References

- Alcácer, A., Epifanio, I., Gual-Arnau, X., 2024. Biarchetype analysis: Simultaneous learning of observations and features based on extremes. IEEE Transactions on Pattern Analysis and Machine Intelligence 46, 8228–8239.
- Alcácer, A., Epifanio, I., Mair, S., Mørup, M., 2025. A survey on archetypal analysis. arXiv preprint arXiv:2504.12392.
- Alcácer, A., Epifanio, I., Valero, J., Ballester, A., 2021. Combining classification and user-based collaborative filtering for matching footwear size. Mathematics 9.
- Bocci, L., Vicari, D., 2024. A clustering model for three-way asymmetric proximities: Unveiling origins and destinations. Symmetry 16, 752.
- Borg, I., Groenen, P.J., 2005. Modern multidimensional scaling: Theory and applications. Springer.
- Bove, G., Okada, A., 2018. Methods for the analysis of asymmetric pairwise relationships. Advances in Data Analysis and Classification 12, 5–31.

- Bove, G., Okada, A., Vicari, D., 2021. Methods for the analysis of asymmetric proximity data. Springer.
- Carroll, D., Arable, P., 1980. Multidimensional scaling. Annual Review of Psychology 31, 607–649.
- Carroll, J.D., Chang, J.J., 1970. Analysis of individual differences in multidimensional scaling via an n-way generalization of "eckart-young" decomposition. Psychometrika 35, 283–319.
- Chaturvedi, A., Carroll, J.D., 1994. An alternating combinatorial optimization approach to fitting the indclus and generalized indclus models. Journal of Classification 11, 155–170.
- Corsten, L.C.A., Gabriel, K.R., 1976. Graphical exploration in comparing variance matrices. Biometrics 32, 851–863.
- Cutler, A., Breiman, L., 1994. Archetypal Analysis. Technometrics 36, 338–347.
- Daigle, G., Rivest, L.P., 1992. A robust biplot. Canadian Journal of Statistics 20, 241–255.
- Di Nuzzo, C., Vicari, D., Vitozzi, A., 2025. A Candecomp/Parafac approach for visualizing flows of asymmetric proximity matrices, in: Scientific Meeting of the Italian Statistical Society, Springer. pp. 159–164.
- D'Enza, A.I., Schisa, V., Palumbo, F., 2021. Principal component analysis for interval data: common approaches and variations. Statistica Applicata-Italian Journal of Applied Statistics 3, 249–270.
- Epifanio, I., 2013. h-plots for displaying nonmetric dissimilarity matrices. Statistical Analysis and Data Mining 6, 136–143.
- Epifanio, I., 2014. Mapping the asymmetrical citation relationships between journals by h-plots. Journal of the Association for Information Science and Technology 65, 1293–1298.
- Epifanio, I., Gimeno, V., Gual-Arnau, X., Ibáñez-Gual, M.V., 2023. Archetypal curves in the shape and size space: Discovering the salient features of curved big data by representative extremes. La Matematica 2, 635–658.

- Epifanio, I., Ibáñez, M.V., Simó, A., 2020. Archetypal analysis with missing data: see all samples by looking at a few based on extreme profiles. The American Statistician 74, 169–183.
- Epifanio, I., Ibáñez, M.V., Simó, A., 2018. Archetypal shapes based on land-marks and extension to handle missing data. Advances in Data Analysis and Classification 12, 705–735.
- Eugster, M.J., Leisch, F., 2009. From Spider-Man to Hero Archetypal Analysis in R. Journal of Statistical Software 30, 1–23.
- Ferrer, R., Benítez, R., Bolós, V.J., 2021. Interdependence between green financial instruments and major conventional assets: a wavelet-based network analysis. Mathematics 9, 900–919.
- Gómez-Sánchez, A., Vitale, R., Ruckebusch, C., de Juan, A., 2024. Solving the missing value problem in PCA by orthogonalized-alternating least squares (O-ALS). Chemometrics and Intelligent Laboratory Systems 250, 105153.
- Groenen, P., Winsberg, S., Rodriguez, O., Diday, E., 2006. I-scal: Multi-dimensional scaling of interval dissimilarities. Computational Statistics & Data Analysis 51, 360–378.
- Groenen, P.J., Winsberg, S., 2006. Multidimensional scaling of histogram dissimilarities, in: Data science and classification. Springer, pp. 161–170.
- Kaufman, L., Rousseeuw, P.J., 1990. Finding Groups in Data: An Introduction to Cluster Analysis. John Wiley, New York.
- Maechler, M., Rousseeuw, P., Struyf, A., Hubert, M., Hornik, K., 2025. cluster: Cluster Analysis Basics and Extensions. URL: https://CRAN.R-project.org/package=cluster.
- Nadler, B., Lafon, S., Coifman, R.R., Kevrekidis, I.G., 2006. Diffusion maps, spectral clustering and reaction coordinates of dynamical systems. Applied and Computational Harmonic Analysis 21, 113–127.
- Okada, A., Imaizumi, T., 1997. Asymmetric multidimensional scaling of two-mode three-way proximities. Journal of Classification 14, 195–224.

- Okada, A., Imaizumi, T., 2024. Applied Multidimensional Scaling of Asymmetric Relationships. Springer.
- Okada, A., Yokoyama, S., 2015. Asymmetric cluster analysis based on skew-symmetry: Acluskew, in: Advances in statistical models for data analysis. Springer, pp. 191–199.
- Okada, A., Yokoyama, S., 2025. Analysis of cultural participation by two-mode three-way asymmetric cluster analysis and multidimensional scaling, in: Advances in Quantitative Approaches to Sociological Issues. Springer, pp. 115–139.
- Olszewski, D., 2016. Asymmetric k-means clustering of the asymmetric self-organizing map. Neural Processing Letters 43, 231–253.
- Olszewski, D., 2023. An asymmetric topology-preserving neighborhood retrieval visualizer. Expert Systems with Applications 225, 120175.
- Olszewski, D., 2024. Asymmetric Isomap for dimensionality reduction and data visualization, in: International Conference on Artificial Neural Networks, Springer. pp. 102–115.
- Podani, J., Miklós, I., 2002. Resemblance coefficients and the horseshoe effect in principal coordinates analysis. Ecology 83, 3331–3343.
- R Development Core Team, 2025. R: A Language and Environment for Statistical Computing. R Foundation for Statistical Computing. URL: http://www.R-project.org. ISBN 3-900051-07-0.
- Roweis, S.T., Saul, L.K., 2000. Linear embedding nonlinear dimensionality reduction by locally. Science 290, 2323–2326.
- Schwarz, A., Karlsson, L., 2019. Scalable eigenvector computation for the non-symmetric eigenvalue problem. Parallel Computing 85, 131–140.
- Seber, G., 1984. Multivariate observations. John Wiley.
- Tenenbaum, J.B., de Silva, V., Langford, J.C., 2000. A global geometric framework for nonlinear dimensionality reduction. Science 290, 2319–2323.

- Thurau, C., Kersting, K., Wahabzada, M., Bauckhage, C., 2012. Descriptive matrix factorization for sustainability: Adopting the principle of opposites. Data Mining and Knowledge Discovery 24, 325–354.
- Torrence, C., Webster, P.J., 1999. Interdecadal Changes in the ENSO–Monsoon System. Journal of Climate 12, 2679–2690.
- Vinué, G., Epifanio, I., 2017. Archetypoid analysis for sports analytics. Data Mining and Knowledge Discovery 31, 1643–1677.
- Vinué, G., Epifanio, I., Alemany, S., 2015. Archetypoids: A new approach to define representative archetypal data. Computational Statistics & Data Analysis 87, 102-115.

Social group	ACLU	SKEW	$ ext{H-plot} +  ext{PAM}$				
	Cluster 1	Cluster 2	Cluster 1	Cluster 2			
Female ju- nior high school grad- uates	Tabloid, Classic, Mu- seum, Lessons, Abroad, Volun- teer, Library, Karaoke	Novels	Abroad, Lessons, Volun- teer	Library, Classic, Museum, Novels, Karaoke, Tabloid			
Female high school grad- uates	Tabloid, Museum, Lessons, Abroad, Volunteer, Library, Karaoke	Novels, Classic	Abroad, Lessons, Volun- teer	Novels, Classic, Museum, Library, Karaoke, Tabloid			
Female ju- nior college or technical college grad- uates	Tabloid, Lessons, Abroad, Li- brary, Karaoke	Novels , Classic, Museum, Volunteer	Abroad, Lessons, Volun- teer	Novels, Classic, Museum, Library, Karaoke, Tabloid			
Female college grad- uates	Tabloid	Novels, Classic, Museum, Lessons, Abroad, Volunteer, Library, Karaoke	Abroad, Classic, Lessons, Volunteer	Novels, Museum, Library, Karaoke, Tabloid			
Male junior high school graduates	Tabloid, Classic, Museum, Lessons, Abroad, Volunteer, Library, Karaoke	Novels	Lessons, Classic, Abroad, Volunteer	Novels, Museum, Library, Karaoke, Tabloid			
Male high school grad- uates	Tabloid, Classic, Mu- seum, Lessons, Abroad, Volun- teer, Library, Karaoke	Novels	Abroad, Classic, Lessons, Volunteer	Novels, Museum, Library, Karaoke, Tabloid			
Male junior college graduates or above	Tabloid	Novels, Classic, Mu- seum, Lessons, Abroad, Volun- teer, Library, Karaoke	Abroad, Classic, Lessons, Volunteer	Library, Museum, Novels, Karaoke, Tabloid			

Table 5: Clustering results for ACLUSKEW and h-plot+PAM for Cultural Participation Data, with two groups.